

Potential Impact of Land-Use Changes on River Basin Hydraulic Parameters Subjected to Rapid Urbanization

Yelbek UTEPOV*, Aleksej ANISKIN, Timoth MKILIMA, Zhanbolat SHAKHMOV, Goran KOZINA

Abstract: Urbanization is a significant challenge that catchments face around the world leading to difficulty in implementing stormwater-related engineering solutions. This study aimed at investigating the impact of land use/land cover change on hydraulic parameters of a rapidly urbanizing river basin, a case of the Jangwani basin in Dar es Salaam, Tanzania. In this study, the peak discharges were estimated using the SCS-Curve Number Method under the combination of ArcGIS and HEC HMS for three different years (1998, 2009, and 2018). The 100-year rainfall event recorded in 2011 was used to develop the meteorological model in HEC HMS. The steady flow analysis was accomplished using the HEC-RAS software package. To capture the effect of land use/land cover change as well as avoiding variability, the same rainfall dataset was applied for all the three study years. According to the modelling results in HEC RAS, the parameters such as top flow width, average velocity, hydraulic depth, conveyance, shear, stream power as well as the cumulative volume were observed to be increasing with time.

Keywords: channel flow; flood mapping; HEC-RAS model; steady flow analysis; urban catchment

1 INTRODUCTION

Urbanization plays a significant role in the loss of vegetation and soils. The vegetation is important for holding down the soil, and it also protects the soil from being washed away during heavy rains. But, when the vegetation is removed, rainwater simply rushes to the lowest point within a catchment, where it accumulates and causes flooding [1]. The general phenomenon makes runoff travel faster to reach streams and in greater quantities. In this case, flooding will occur sooner and in a more severe extent in comparison to the scenario when precipitation falls on the natural ground surface. Flood is a natural hazard resulting from water overflowing above the normal occurrence in which it submerges the normally dry land. Floods account for many deaths around the globe every year [2]. The arrogant nature of floods has not only been impacting the developing countries but also the developed countries are under significant pressure of flooding incidents [3-5]. The complex phenomenon of a flood event makes it very difficult to accurately predict [6], which in turn affects the planning of control measures. In recent years where the advancement of technology has been observed, there is no doubt that the use of resources developed through Geographical Information Systems (GIS) and Remote Sensing (RS) in conjunction with other resources gives a handful way of identifying, monitoring and assessment of natural disasters including floods [7], [8]. With being a global challenge, many engineering studies have been conducted to investigate different behavioral characteristics of floods [9-14].

Land surface cover (extent of imperviousness) plays a significant role in the characteristics of stormwater runoff and flood events in general [15]. Increased impervious surface area is a consequence of urbanization, which has significant effects on the hydrological system of a catchment. The increase in impervious surface leads to shorter lag times between onset of precipitation and subsequently higher runoff peaks as well as the total volume of runoff in receiving stream exceeding the design capacity of the particular stream [16]. Previous studies have shown the general relationship between land surface cover and stormwater runoff generated [17, 18]. However,

the degree at which land use/land cover change impacts individual hydraulic parameters of a catchment over time has not been widely captured. The present study focuses on investigating the response of hydraulic parameters in a river basin subjected to rapid urbanization.

Moreover, a lack of observed data is one of the challenges during the flood mapping processes in ungauged catchments or basins, [19]. Modeling is a promising approach used in the estimation of design peak discharges for ungauged basins [20, 21]. However, there are still some challenges for the models to accurately represent the real physical situation [22]. The combination of Soil Conservation Service Curve Number (SCS-CN) method for land surface characterization, Hydrologic Modeling System (HEC-HMS) for hydrologic modeling as well as flow analysis using the USACE Hydrologic Engineering Center's River Analysis System (HEC RAS) is one of the useful approaches to help engineers in the flood inundation processes [23, 24].

The SCS curve number method is regarded to be a simple, widely used and efficient method for the estimation of stormwater runoff from a rainfall event in a particular area, while HEC-HMS is hydrological software designed to simulate the complete hydrologic processes of a catchment. Moreover, HEC-RAS is a combined system of software with several components including a graphical user interface (GUI), hydraulic analysis components, data storage and management capabilities, graphics, and reporting facilities [25].

For many years now, Dar es Salaam is under the pressure of flooding incidents [26], and the Jangwani basin located within the Msimbazi is part of the rapidly urbanizing and flood-affected areas in the city. In December 2011, Dar es Salaam was hit with the worst flooding from an extreme event to be recorded since the 1950s. According to the Tanzania Red Cross, the floods resulted in 41 fatalities, injured over 200 people, displaced 10000 people, and affected an estimated 50000 people. 2500 people were reported to be missing. Also, 680 temporary shelters were constructed to accommodate the 3400 of the displaced [27].

In this study, the HEC-RAS software package is used for flood mapping and analysis for a case of the Jangwani

basin in Dar es salaam, Tanzania. The objective of this study is to investigate the response of the basin hydraulic parameters to the changing flow characteristics as induced by the rapid urbanization within the catchment. The question of the study is based on how land use/land cover has been affecting the hydraulic parameters in the basin. Nearest neighbor catchment approach was used for the hydrological model validation, as the study catchment is ungauged. Parameters such as total elevation of the energy grade line, average velocity of flow in the total cross-section, conveyance of the total cross-section, stream power as well as shear stress are investigated.

2 MATERIALS AND METHODS

2.1 Case Study Description

The Jangwani basin which is part of the Msimbazi catchment is located in Dar es Salaam, Tanzania, which is the most populated city in the country (Fig. 1). The basin is located between latitudes 6°27' and 7°15' south of the Equator and between longitudes 39° and 39°33' East of Greenwich. It is the most downstream sub-catchment of the Mzimbazi river with its origin in the Kisarawe hills (forests) and flows across the Dar es Salaam discharging water to the Indian Ocean with more than 36 kilometers [28].

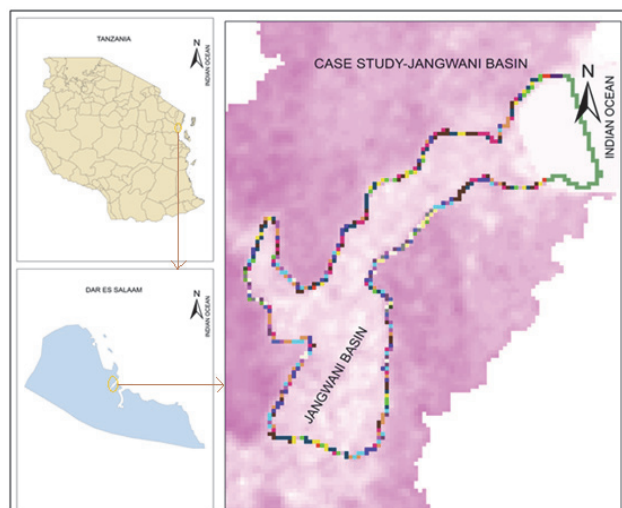


Figure 1 Case study

The basin is characterized by recurring flood events almost every rainy season, which is among the fastest-growing and most rapidly urbanizing areas. Rapid urbanization in the city has also increased pressure in the basin as there are many development activities taking place within the catchment including the establishment of settlements. Generally, the city receives a mean annual rainfall of more than 1400 mm/year [29], with two wet seasons, short rains from November to January, and long rains from March to May. The period of January and February constitutes the short dry season with the long dry season lasting from late June to mid-October. Temperatures in Dar es Salaam can get as high as 104 °F (40 °C).

2.2 Datasets

This study used a Digital Elevation Model (DEM) obtained from the official website of the United States Geological Survey with 30 m by 30 m resolution and then clipped to the extent of the case study using a prepared shapefile of the catchment in ArcGIS 10.5 for the development of the Triangular Irregular Network (TIN) in HEC RAS. A 100-year rainfall event recorded by the Tanzania Meteorological Agency (TMA) in 2011 was used for flow computations. The peak discharges estimated using the SCS Curve Number method in ArcGIS and HEC HMS for study years 1998, 2009, and 2018 were used in HEC RAS for steady flow analysis. The results were then validated by the polygons and points of the known locations which are highly impacted by flood events extracted from the high-resolution Google Earth images.

2.3 Methodology

Because the catchment is ungauged, modeling of the peak discharges was necessary. The input datasets to the HEC HMS model were processed in the ArcGIS 10.5 software package. The quantified peak discharges for the three study years were then used for steady flow analysis in HEC RAS.

2.3.1 Stormwater Runoff Modeling

In ArcGIS, DEM was used to delineate the catchment as well as extracting the physical characteristics of the streams. The Basin Characteristics tool of HEC-GeoHMS was used to extract river length, river slope, basin slope, longest flow path, basin centroid, basin centroid elevation as well as the centroidal longest flow path.

For the utilization of the SCS-CN method, several procedures were executed in ArcGIS, which includes: processing of Landsat images, soil data processing, merging of classified land uses with soil data as well as creating CN Lookup table. The *CN* value can be estimated by using the SCS equation for the potential maximum retention (Eq. (1)).

$$CN = \frac{254000}{S + 254} \quad (1)$$

where *S* is the maximum retention capacity of the soil, mm [30].

In this study, the CN Lag Method function was used to compute basin lag in hours in which is the weighted time of concentration or time computed from the center of mass of excess rainfall hyetograph to the peak of storm runoff hydrograph. The datasets from ArcGIS were exported to HEC HMS where a Meteorological Model was created based on the daily rainfall data collected from the Tanzania Meteorological Agency (TMA). The 100-year extreme event recorded in December 2011 was selected and used for the development of the Meteorological model in HEC HMS.

The SCS derived the following equation to calculate *Q* (2).

$$Q = \frac{(P - 0,2S)^2}{P + 0,8S} \quad (2)$$

where Q is runoff depth, mm; P is daily rainfall, mm.

However, as can be seen in Eq. (2), its application requires the maximum retention capacity (S) to be estimated. The S is a function of the CN and its computation is summarized in Eq. (3).

$$S = 254 \left(\frac{100}{CN} - 1 \right) \quad (3)$$

After estimating Q , the Q_r of a rainfall event is also estimated as the product of the Q and the target land surface area on which the rainfall occurred. The calculation of Q_r from Q and the target land surface area is summarized in Eq. (4), [31].

$$Q_r = \left(\frac{Q}{100} \right) A \quad (4)$$

Nearby catchment was used to validate the model coupled with the daily rainfall data from December 2011 extreme event. The model was calibrated using different approaches to determine the most appropriate method for the representation of the study catchment. Apart from having a piece of knowledge about the study catchment, the simulated flows were also investigated statistically.

2.3.2 HEC RAS Flow Analysis

With the help of the HEC RAS software package, the flood mapping was accomplished. Currently, with the release of HEC RAS 5.0.4; the HEC RAS Mapper embedded in HEC RAS removes the necessity of the HEC GeoRAS tool. The procedures in HEC RAS started with data pre-processing by specifying the coordinate system, adding terrain data as well as creating new geometry. The clipped DEM to the catchment size was then converted to a triangulated irregular network (TIN) elevation model, followed by creating the river geometry in RAS Mapper. The process followed by the development of river attributes (river centerline, river banks, river flow paths, river cross-sections (Fig. 2)), and error checking.

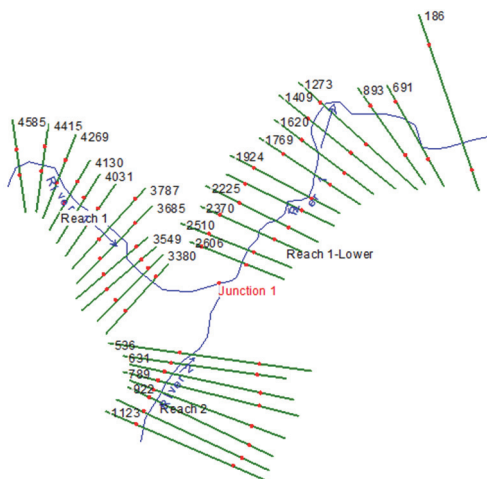


Figure 2 Geometric data

The other procedures were setting roughness coefficients for all the cross-sections. The cross-section profiles should be drawn perpendicular to the direction of river flow, where the calculation of the water level in a given profile relies on the water level computed in the previous profile. As an advancement to the 1D modeling, the 2D model is designed to work with both steady and unsteady flow conditions. In this study, the 1D modeling was achieved through steady-state flow conditions as well as the downstream boundary condition of normal depth (slope) set to 0,006 obtained from the basin elevation profile.

From each cross-section, the water surface extent points are then linearly joined producing the inundation extent. Finally, the model was executed with steady and unsteady analyses, and the results were visualized.

Generally, each cross-section in the HEC-RAS model is defined by several attributes including river, reach, as well as river station. The cross-section geometry is obtained by defining the station and elevation (X-Y data) from left to right, as well as from upstream to downstream direction. Despite the fact that cross-sections can be extracted from a TIN some little adjustments may be needed as TIN does not always define the channel with enough resolution to accurately demarcate a cross-section through the channel. In each cross-section, the locations of the stream banks are identified and used to divide the stream into segments of the left floodway, main channel, and right floodway.

HEC-RAS subdivides the cross-sections in this manner, because of differences in hydraulic parameters. For example, the wetted perimeter in the floodway is much higher than in the main channel. Thus, friction forces between the water and channel bed have a greater influence to flow resistance in the floodway, leading to lower values of the Manning coefficient. As a result, the flow velocity and conveyance are substantially higher in the main channel than in the floodway.

Fig. 3 presents the general summary of the workflow from the primary datasets to the steady flow analysis in HEC RAS. A combination of three main software packages (ArcGIS, HEC HMS, and HEC RAS) was used to accomplish this study, with the steady flow analysis in HEC RAS being the main target of the study.

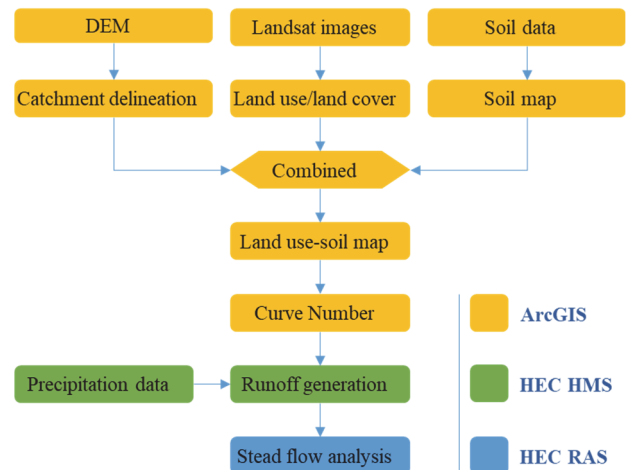


Figure 3 General flowchart

3 RESULTS AND DISCUSSION

To capture the effect of land use/land cover change on the hydraulic parameters of the study basin, the extent to which the land surface has been changing was investigated. The land use/land cover classes were grouped into three main classes, namely: water bodies, forests, developed high intensity, developed medium intensity as well as developed low intensity.

Table 1 Land use/land cover classes from 1998 to 2018

| Type of land use | Land use coverage / % | | |
|-----------------------------|-----------------------|-----------|-----------|
| | Year 1998 | Year 2009 | Year 2018 |
| Water bodies | 0,13 | 0,26 | 0,44 |
| Forest | 8,42 | 14,69 | 1,86 |
| Developed, high intensity | 3,82 | 13,42 | 19,77 |
| Developed, medium intensity | 25,97 | 50,49 | 61,12 |
| Developed, low intensity | 61,67 | 21,13 | 16,82 |
| Total | 100,00 | 100,00 | 100,00 |

From Tab. 1, it can be observed that while the coverage of low-intensity development is decreasing, the coverage of high-intensity development is increasing. From 1998 to 2018 the catchment has observed an increase of 15,95% of high-intensity development with a decrease of 44,85% of low-intensity development coverage. The increase in high-

intensity development can be associated with the development activities in the catchment including the increasing land demand for settlements, roads, industries as well as business centers [32].

Following the hydrologic modeling in HEC HMS that resulted in estimated peak discharges of 355,7 m³/s from 1998 datasets, 402,7 m³/s from 2009 datasets as well as 437,8 m³/s from 2018 datasets, the steady flow analysis in HEC RAS was accomplished. The increase of peak discharges from 1998 to 2018 is approximately 23,08%. The performed steady flow analysis was able to produce water surface profiles as well as the extents of each flood plain in the study basin. In this study, several input parameters for hydraulic analysis of the stream channel geometry and water flow were used. From the input parameters, a series of cross-sections were developed along the stream in the study basin. Following the steady flow analysis with three different plans differentiated with flow discharges from 1998, 2009 and 2018 datasets, the 1D HEC RAS model (flood mapping) was successfully developed. Fig. 4, represents the selected and extracted cross-sections from three different reaches covered in this study. Despite the challenge with the TIN resolution, the demarcation of the stream boundaries was sufficiently achieved.

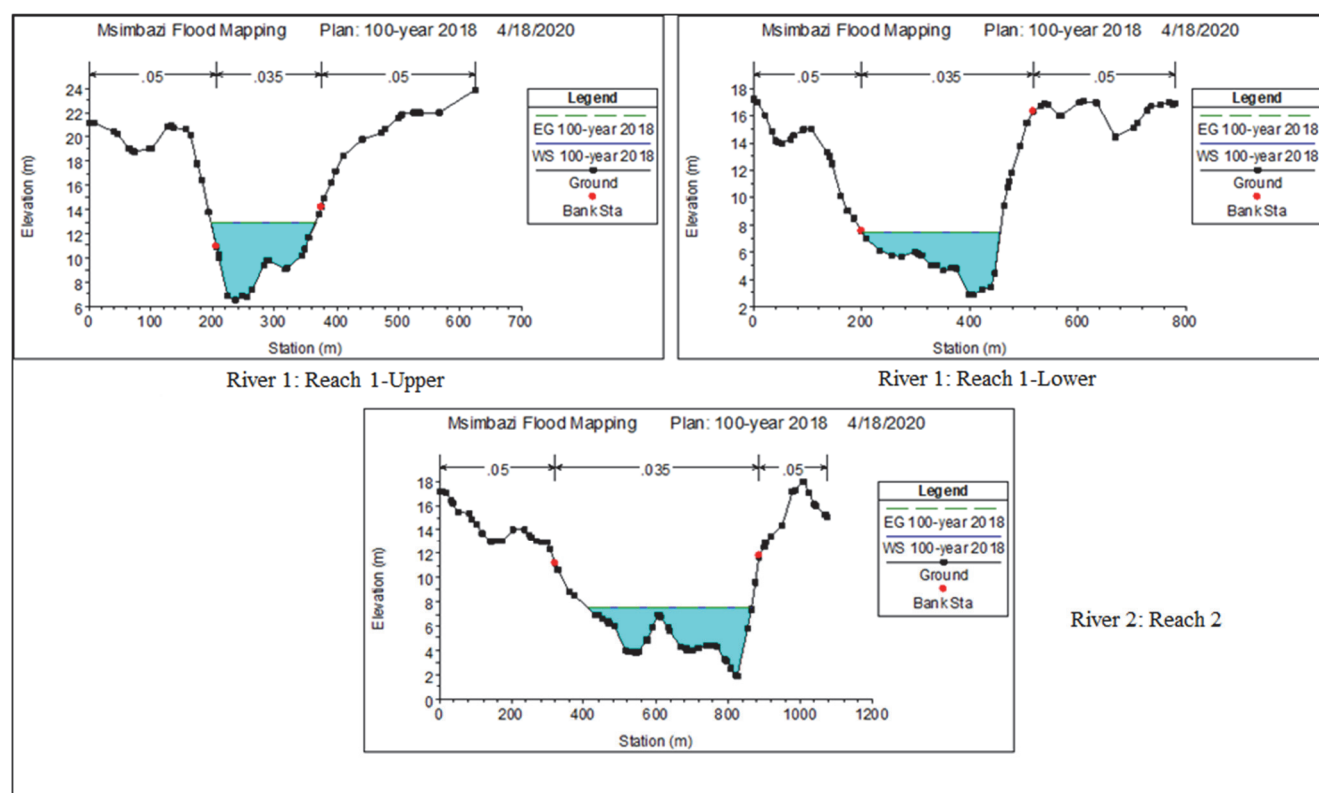


Figure 4 Extracted cross-sections from 2018 plan

From Tabs. 2 to 4, it can be observed that the conveyance of the total cross-section increased with the increase in the total flow. Also, the average velocity of flow in the total cross-section increased from 1998 to 2018 as a result of the change in land use characteristics that in turn affects the quantity of stormwater runoff generated. The 23,08% increase in the peak flow discharge from 1998 to 2018 led to the following results:

- From river 1: reach 1-upper; 2,28% increase in the total elevation of the energy grade line, 13,56%

increase in average velocity of flow in the total cross-section as well as 11,73% increase in the conveyance of the total cross-section.

- From river 1: reach 1-lower; 2,62% increase in the total elevation of the energy grade line, 14,71% increase in average velocity of flow in the total cross-section as well as 7,76% increase in the conveyance of the total cross-section.
- From river 2: reach 2; 2,9% increase in the total elevation of the energy grade line, 10 % increase in the

average velocity of flow in the total cross-section as well as 13,5% increase in the conveyance of the total cross-section.

The phenomenon can be highly linked to the fact that, in urban areas, where there is an increase in land, surface is covered by roads and buildings, they have less capacity to store stormwater. Development activities often involve removing vegetation, soil, and depressions from the land surface. The permeable soil is replaced by impermeable surfaces such as roads, roofs, parking lots, and sidewalks that store little water, reduce infiltration of water into the ground, and accelerate runoff to ditches and streams [33].

Table 2 Cross-sections hydraulic outputs for 1998 plan

| Element | Plan: 100-year 1998 | | |
|---------------------------------|---------------------|----------------|----------|
| | R1 : R1: Upper | R1 : R1: Lower | R2 : R2 |
| E. G. Elev / m | 12,71 | 7,25 | 7,27 |
| W. S. Elev / m | 12,69 | 7,24 | 7,27 |
| E. G. Slope / m/m | 0,000072 | 0,000023 | 0,000015 |
| Q Total / m ³ /s | 355,7 | 355,7 | 355,7 |
| Top Width / m | 165,68 | 275,21 | 739,05 |
| Vel Total / m/s | 0,59 | 0,34 | 0,2 |
| Max Chl Dpth / m | 6,16 | 6,24 | 5,36 |
| Conv. Total / m ³ /s | 41838,1 | 74297,9 | 91854,8 |
| Min Ch El / m | 6,53 | 1 | 1,91 |
| Alpha | 1,01 | 1 | 1,04 |

Table 3 Cross-sections hydraulic outputs for 2009 plan

| Element | Plan: 100-year 2009 | | |
|---------------------------------|---------------------|----------------|----------|
| | R1 : R1: Upper | R1 : R1: Lower | R2 : R2 |
| E. G. Elev / m | 12,88 | 7,37 | 7,4 |
| W. S. Elev / m | 12,86 | 7,36 | 7,4 |
| E. G. Slope / m/m | 0,000081 | 0,000027 | 0,000016 |
| Q Total / m ³ /s | 402,7 | 402,7 | 402,7 |
| Top Width / m | 167,76 | 277,29 | 743,31 |
| Vel Total / m/s | 0,63 | 0,37 | 0,21 |
| Max Chl Dpth / m | 6,33 | 6,36 | 5,49 |
| Conv. Total / m ³ /s | 44670,2 | 77757,1 | 99240,9 |
| Min Ch El / m | 6,53 | 1 | 1,91 |
| Alpha | 1,02 | 1 | 1,04 |

Table 4 Cross-sections hydraulic outputs for 2018 plan

| Element | Plan: 100-year 2018 | | |
|---------------------------------|---------------------|----------------|----------|
| | R1 : R1: Upper | R1 : R1: Lower | R2 : R2 |
| E. G. Elev / m | 13 | 7,44 | 7,48 |
| W. S. Elev / m | 12,97 | 7,44 | 7,48 |
| E. G. Slope / m/m | 0,000088 | 0,00003 | 0,000018 |
| Q Total / m ³ /s | 437,8 | 437,8 | 437,8 |
| Top Width / m | 169,25 | 278,66 | 746,12 |
| Vel Total / m/s | 0,67 | 0,39 | 0,22 |
| Max Chl Dpth / m | 6,44 | 6,44 | 5,57 |
| Conv. Total / m ³ /s | 46747,6 | 80066,2 | 104255,2 |
| Min Ch El / m | 6,53 | 1 | 1,91 |
| Alpha | 1,02 | 1 | 1,04 |

Where: E. G. Elev - the elevation of the energy grade line in the given profile, m; W. S. Elev - water surface elevation, m; E. G. Slope - slope of the energy grade line; Vel Total - average velocity of flow in the total cross-section; Max Chl Dpth - maximum main channel depth, m; Conv. Total - conveyance of the total cross-section; Length Wtd - weighted cross-section reach length, based on flow distribution, in the left bank, channel, and right bank; Min Ch El - minimum channel elevation, m; the lowest bed elevation; Alpha - alpha energy weighting coefficient.

From the modeling results, it can be observed that the area of flow for reach-1-upper, reach-1-lower as well as reach-2 has been increasing with time as a result of the change in land use/land cover (Tabs. 5 to 7). A similar

phenomenon can be observed for all the other parameters such as top flow width, average velocity, hydraulic depth, conveyance, shear, stream power as well as the cumulative volume.

Table 5 Computed flow parameters for river1-reach-1-upper

| Element | River 1-reach 1-Upper | | |
|----------------------------------|-----------------------|----------|----------|
| | Year1998 | Year2009 | Year2018 |
| Flow Area / m ² | 601,14 | 627,2 | 645,97 |
| Area / m ² | 601,14 | 627,2 | 645,97 |
| Flow / m ³ /s | 354,64 | 401,28 | 436,08 |
| Top Width / m | 158,03 | 159,4 | 160,39 |
| Avg. Vel. / m/s | 0,59 | 0,64 | 0,68 |
| Hydr. Depth / m | 3,8 | 3,93 | 4,03 |
| Conv. / m ³ /s | 41714 | 44513,2 | 46564,1 |
| Wetted Per. / m | 158,83 | 160,21 | 161,2 |
| Shear / N/m ² | 2,68 | 3,12 | 3,45 |
| Stream Power / N/m·s | 1,58 | 2 | 2,33 |
| Cum Volume / 1000 m ³ | 1224 | 1271,94 | 1305,65 |
| Cum SA / 1000 m ² | 211,65 | 215,41 | 217,87 |

From the upper section of the first reach of the study basin, an increase of 7,46% of flow can be observed from 1998 to 2018 (Tab. 5). Also, from the lower section of the first reach, an increase of 5,11% of the flow area was observed from 1998 to 2018. Moreover, an 8.18% increase was observed from the second reach of the study basin from 1998 to 2018, making the general average percent increase of flow area for the entire study basin be 6,92% from 1998 to 2018. With the fact that the basin is one of the low-lying areas and densely populated, even a small increase in flow area can be of significant threat [34]. Therefore, the observed increase in flow area can be highly linked to the elevating disastrous flooding events within the catchment.

Also, an increase of 58,62% of stream power from 1998 to 2018 was observed from reach-1-lower located downstream of the three reaches, 57,14% from reach-2 as well as 47,47% from reach-1-upper. With the increase in stream power, the studied reaches are prone to an increasing rate of soil erosion. According to [35], it was observed that stream power has a significant potential to erosion within a river reach.

The minimum shear increase of 9,52% was observed from 2009 to 2018 from reach 2, with 28,73% being the maximum shear increase which was observed from the reach-1-upper from 1998 to 2018.

Table 6 Computed flow parameters for river 1-reach-1-lower

| Element | River 1-reach 1-Lower | | |
|----------------------------------|-----------------------|-----------|-----------|
| | Year 1998 | Year 2009 | Year 2018 |
| Flow Area / m ² | 1060,03 | 1092,68 | 1114,24 |
| Area / m ² | 1060,03 | 1092,68 | 1114,24 |
| Flow / m ³ /s | 355,7 | 402,7 | 437,8 |
| Top Width / m | 275,21 | 277,29 | 278,66 |
| Avg. Vel. / m/s | 0,34 | 0,37 | 0,39 |
| Hydr. Depth / m | 3,85 | 3,94 | 4 |
| Conv. / m ³ /s | 74297,9 | 77757,1 | 80066,2 |
| Wetted Per. / m | 275,88 | 277,98 | 279,36 |
| Shear / N/m ² | 0,86 | 1,03 | 1,17 |
| Stream Power / N/m·s | 0,29 | 0,38 | 0,46 |
| Cum Volume / 1000 m ³ | 924,01 | 983,57 | 1023,05 |
| Cum SA / 1000 m ² | 703,65 | 728,9 | 736,89 |

In general, the change in land use/land cover is observed to be affecting the stormwater runoff characteristics which in turn affect the flow regimes as well as the basin at large. In the literature, the Spatio-temporal variability of land use/land cover change within a

catchment is also observed to be one of the significant factors affecting flow regimes of a river [36].

Table 7 Computed flow parameters for river 2-reach-2

| Element | River 2-reach 2 | | |
|----------------------------------|-----------------|-----------|-----------|
| | Year 1998 | Year 2009 | Year 2018 |
| Flow Area / m ² | 1605,89 | 1684,83 | 1737,21 |
| Area / m ² | 1605,89 | 1684,83 | 1737,21 |
| Flow / m ³ /s | 327,33 | 370,47 | 402,67 |
| Top Width / m | 641,6 | 644,44 | 646,32 |
| Avg. Vel. / m/s | 0,2 | 0,22 | 0,23 |
| Hydr. Depth / m | 2,5 | 2,61 | 2,69 |
| Conv. / m ³ /s | 84528,8 | 91297,2 | 95890,2 |
| Wetted Per. / m | 642,21 | 645,06 | 646,94 |
| Shear / N/m ² | 0,37 | 0,42 | 0,46 |
| Stream Power / N/m·s | 0,07 | 0,09 | 0,11 |
| Cum Volume / 1000 m ³ | 1122,02 | 1171,69 | 1204,79 |
| Cum SA / 1000 m ² | 292,96 | 296,74 | 299,69 |

Where: Hydr. Depth - hydraulic depth for cross-section (area/top-width of active flow); Conv - conveyance; Cum Volume - cumulative volume; Cum SA - cumulative surface area.

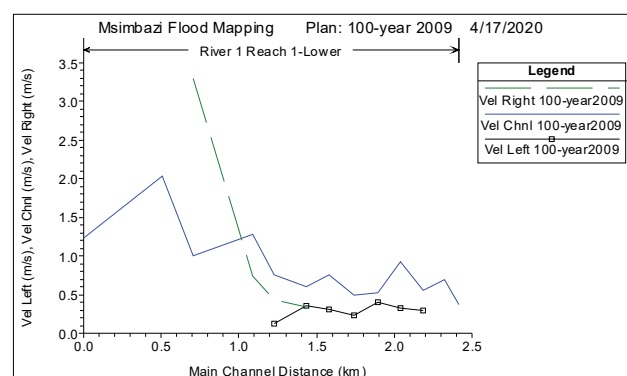


Figure 5 General profile plot (distance vs velocity)

From Fig. 5 it can be observed that the flow velocity in the basin decreases towards the downstream which is characterized by relatively flat surfaces.

4 CONCLUSIONS

The potential effect of the land use/land cover change on hydraulic parameters of a rapidly urbanizing and ungauged river basin has been investigated. GIS-based techniques were used to investigate the trend of land use/land cover change within the study basin. The SCS-Curve number approach was used for storm water runoff modelling and computation of peak discharges in HEC HMS, which were then used for hydraulic modelling in HEC RAS. From the land use/land cover analysis, the study observed one of 15,95% of high-intensity developed areas with a decrease of 44,85% of low-intensity developed areas. The increase in high-intensity developed areas has a significant contribution to the increase in impervious surfaces affecting the behaviour and characteristics of the generated runoff. As a result of the change in land use/land cover, the study basin observed an increase of 23,08% of peak discharge from 1998 to 2018.

The modelling results in HEC RAS revealed potential changes in hydraulic parameters within the study catchment where most of the parameters such as top flow width, average velocity, hydraulic depth, conveyance, shear, stream power as well as the cumulative volume were

observed to be increasing with time. For example, the increase in the total elevation of the energy grade line was observed to be ranging from 2,28 to 2,9% from 1998 to 2018. The velocity of flow in the total cross-section ranged from 10 to 14,71% while the conveyance of the total cross-section ranged from 7,76 to 13,5%.

The results derived from this study, provide a piece of useful information through awareness of the potential relationship between the changes in a land surface cover that in turn affect the flow characteristics in a catchment or basin. Also, this information can be useful for proper basin management planning. However, this study used the Jangwani basin, which is a sub-catchment of the Msimbazi River, but it would be interesting for future studies to focus on understanding how the entire catchment responds to the rapid urbanization as well as how each sub-catchment (basin) responds when the whole catchment is incorporated.

Acknowledgements

This research was funded by the Science Committee of the Ministry of Education and Science of the Republic of Kazakhstan (Grant No. AP09258790).

5 REFERENCES

- [1] Mohammad, A. G. & Adam, M. A. (2010). The impact of vegetative cover type on runoff and soil erosion under different land uses. *CATENA*, 81(2), 97-103. <https://doi.org/10.1016/j.catena.2010.01.008>
- [2] Alderman, K., Turner, L. R., & Tong, S. (2012). Floods and human health: A systematic review. *Environment International*, 47, 37-47. <https://doi.org/10.1016/j.envint.2012.06.003>
- [3] Salami, R. O., Von Meding, J. K., & Giggins, H. (2017). Urban settlements' vulnerability to flood risks in African cities: A conceptual framework. *Jamba: Journal of Disaster Risk Studies*, 9(1). <https://doi.org/10.4102/jamba.v9i1.370>
- [4] Osti, R., Tanaka, S., & Tokioka, T. (2008). Flood hazard mapping in developing countries: Problems and prospects. *Disaster Prevention and Management. An International Journal*. <https://doi.org/10.1108/09653560810855919>
- [5] Doocy, S., Daniels, A., Murray, S., & Kirsch, T. D. (2013). The Human Impact of Floods: a Historical Review of Events 1980-2009 and Systematic Literature Review. *PLoS Currents*. <https://doi.org/10.1371/currents.dis.f4deb457904936b07c09daa98ee8171a>
- [6] Moore, R. J., Bell, V. A., & Jones, D. A. (2005). Forecasting for flood warning. *Comptes Rendus Geoscience*, 337(1-2), 203-217. <https://doi.org/10.1016/j.crte.2004.10.017>
- [7] Dewan, A. M., Islam, M. M., Kumamoto, T., & Nishigaki, M. (2007). Evaluating Flood Hazard for Land-Use Planning in Greater Dhaka of Bangladesh Using Remote Sensing and GIS Techniques. *Water Resources Management*, 21(9), 1601-1612. <https://doi.org/10.1007/s11269-006-9116-1>
- [8] Lawal, D. U., Matori, A. N., Hashim, A. M., Chandio, I. A., Sabri, S., Balogun, A. L., & Abba, H. A. (2011). Geographic information system and remote sensing applications in flood hazards management: A review.
- [9] Munoz, S. E., Giosan, L., Therrell, M. D., Remo, J. W. F., Shen, Z., Sullivan, R. M., Wiman, C., O'Donnell, M., & Donnelly, J. P. (2018). Climatic control of Mississippi River flood hazard amplified by river engineering. *Nature*, 556(7699), 95-98. <https://doi.org/10.1038/nature26145>
- [10] Thurman, J. T. (2014). *Flood Control and Drainage Engineering*. CRC Press. <https://doi.org/10.1201/b16514>
- [11] Xu, G., Huang, G. Q., & Fang, J. (2015). Cloud asset for

- urban flood control. *Advanced Engineering Informatics*, 29(3), 355-365. <https://doi.org/10.1016/j.aei.2015.01.006>
- [12] Singh, V. (2016). Hydraulic Engineering. Introduction to Tsallis Entropy Theory in Water Engineering. *CRC Press*. <https://doi.org/10.1201/b19113>
- [13] Lollino, G., Arattano, M., Rinaldi, M., Giustolisi, O., Marechal, J. C., & Grant, G. E. (2015). *Engineering Geology for Society and Territory - Volume 3*. Springer International Publishing. Cham. https://doi.org/10.1007/978-3-319-09060-3_134
- [14] Ren, M., He, X., Kan, G., Wang, F., Zhang, H., Li, H., Cao, D., Wang, H., Sun, D., Jiang, X., Wang, G., & Zhang, Z. (2017). A Comparison of Flood Control Standards for Reservoir Engineering for Different Countries. *Water*, 9(3), 152. <https://doi.org/10.3390/w9030152>
- [15] Guzha, A. C., Rufino, M. C., Okoth, S., Jacobs, S., & Nóbrega, R. L. B. (2018). Impacts of land use and land cover change on surface runoff, discharge and low flows: Evidence from East Africa. *Journal of Hydrology: Regional Studies*, 15, 49-67. <https://doi.org/10.1016/j.ejrh.2017.11.005>
- [16] Shuster, W. D., Bonta, J., Thurston, H., Warnemuende, E., & Smith, D. R. (2005). Impacts of impervious surface on watershed hydrology: A review. *Urban Water Journal*, 2(4), 263-275. <https://doi.org/10.1080/15730620500386529>
- [17] Githui, F., Mutua, F., & Bauwens, W. (2009). Estimating the impacts of land-cover change on runoff using the soil and water assessment tool (SWAT): case study of Nzoia catchment, Kenya / Estimation des impacts du changement d'occupation du sol sur l'écoulement à l'aide de SWAT: étude du cas du bassin. *Hydrological Sciences Journal*, 54(5), 899-908. <https://doi.org/10.1623/hysj.54.5.899>
- [18] Sriwongsitanon, N. & Taesombat, W. (2011). Effects of land cover on runoff coefficient. *Journal of Hydrology*, 410(3-4), 226-238. <https://doi.org/10.1016/j.jhydrol.2011.09.021>
- [19] Vojtek, M., Petroselli, A., Vojteková, J., & Asgharinia, S. (2019). Flood inundation mapping in small and ungauged basins: Sensitivity analysis using the EBA4SUB and HEC-RAS modeling approach. *Hydrology Research*, 50(4), 1002-1019. <https://doi.org/10.2166/nh.2019.163>
- [20] Tegegne, G. & Kim, Y. O. (2019). Modelling ungauged catchments using the catchment runoff response similarity. *Journal of Hydrology*, 564, 452-466. <https://doi.org/10.1016/j.jhydrol.2018.07.042>
- [21] Massmann, C. Modelling Snowmelt in Ungauged Catchments. *Water*, 11(2), 301. <https://doi.org/10.3390/w11020301>
- [22] Clark, M. P., Fan, Y., Lawrence, D. M., Adam, J. C., Bolster, D., Gochis, D. J., Hooper, R. P., Kumar, M., Leung, L. R., Mackay, D. S., Maxwell, R. M., Shen, C., Swenson, S. C., & Zeng, X. (2015). Improving the representation of hydrologic processes in Earth System Models. *Water Resources Research*, 51(8), 5929-5956. <https://doi.org/10.1002/2015WR017096>
- [23] Knebl, M. R., Yang, Z. L., Hutchison, K., & Maidment, D. R. (2005). Regional scale flood modeling using NEXRAD rainfall, GIS, and HEC-HMS/RAS: a case study for the San Antonio River Basin Summer 2002 storm event. *Journal of Environmental Management*, 75(4), 325-336. <https://doi.org/10.1016/j.jenvman.2004.11.024>
- [24] Goodell, C. & Warren, C. (2006). Flood Inundation Mapping using HEC-RAS. *Obras y Proyectos*, 18-23.
- [25] Husain, A. (2017). Flood Modelling by using HEC-RAS. *International Journal of Engineering Trends and Technology*, 50(1), 1-7. <https://doi.org/10.14445/22315381/IJETT-V50P201>
- [26] Kiunsi, R. (2013). The constraints on climate change adaptation in a city with a large development deficit: the case of Dar es Salaam. *Environment and Urbanization*, 25(2), 321-337. <https://doi.org/10.1177/0956247813489617>
- [27] International Federation of Red Cross and Red Crescent Societies (2012). Retrieved from <http://www.ifrc.org/what/disasters/responding/drs/tools/dref/donors.asp>.
- [28] Igulu, B. S. & Mshiu, E. E. (2020). Monitoring Impervious Surface Area Dynamics to Assess Urbanisation of a Catchment: Msimbazi River Valley Dar es Salaam, 1989 - 2015. *Tanzania Journal of Science*, 46(2), 254-265.
- [29] Mbuligwe, S. E. & Kaseva, M. E. (2005). Pollution and Self-Cleansing of an Urban River in a Developing Country: A Case Study in Dar es Salaam, Tanzania. *Environmental Management*, 36(2), 328-342. <https://doi.org/10.1007/s00267-003-0068-4>
- [30] Bansode, A. & Patil, K. A. (2014). Estimation of Runoff by using SCS Curve Number Method and Arc GIS. *International Journal of Scientific & Engineering Research*.
- [31] Nhamo, L. & Chilonda, P. (2013). Validation of the rainfall-runoff SCS-CN model in a catchment with limited measured data in Zimbabwe. *International Journal of Water Resources and Environmental Engineering*, 5(6), 295-303.
- [32] Todd, G., Msuya, I., Levira, F., & Moshi, I. (2019). City Profile: Dar es Salaam, Tanzania. *Environment and Urbanization ASIA*, 10(2), 193-215. <https://doi.org/10.1177/0975425319859175>
- [33] Du, J., Cheng, L., Zhang, Q., Yang, Y., & Xu, W. (2019). Different Flooding Behaviors Due to Varied Urbanization Levels within River Basin: A Case Study from the Xiang River Basin, China. *International Journal of Disaster Risk Science*, 10(1), 89-102. <https://doi.org/10.1007/s13753-018-0195-4>
- [34] Bangalore, M., Smith, A., & Veldkamp, T. (2019). Exposure to Floods, Climate Change, and Poverty in Vietnam. *Economics of Disasters and Climate Change*, 3(1), 79-99. <https://doi.org/10.1007/s41885-018-0035-4>
- [35] Bizzi, S. & Lerner, D. N. (2015). The Use of Stream Power as an Indicator of Channel Sensitivity to Erosion and Deposition Processes. *River Research and Applications*, 31(1), 16-27. <https://doi.org/10.1002/rra.2717>
- [36] Lei, C. & Zhu, L. (2018). Spatio-temporal variability of land use/land cover change (LULCC) within the Huron River: Effects on stream flows. *Climate Risk Management*, 19, 35-47. <https://doi.org/10.1016/j.crm.2017.09.002>

Contact information:

Yelbek UTEPOV, PhD, Associate Professor
(Corresponding author)
Department of Civil Engineering,
L. N. Gumilyov Eurasian National University,
010000, Nur-Sultan, Kazakhstan
E-mail: utepov-elbek@mail.ru

Aleksej ANISKIN, PhD, Assistant professor
Department of Civil Engineering, University North,
42000 Varaždin, Croatia
E-mail: aaniskin@unin.hr

Timoth MKILIMA, MSc, PhD Candidate
Department of Civil Engineering,
L. N. Gumilyov Eurasian National University,
010000, Nur-Sultan, Kazakhstan
E-mail: tmkilima@gmail.com

Zhanbolat SHAKHMOV, PHD
Department of Civil Engineering,
L. N. Gumilyov Eurasian National University,
010000, Nur-Sultan, Kazakhstan
E-mail: zhanbolat8624@mail.ru

Goran KOZINA, PhD, Full Professor
University North,
42000 Varaždin, Croatia
E-mail: goran.kozina@unin.hr